Digital filters for coherent optical receivers

Seb J. Savory

Optical Networks Group, Dept. of Electronic & Electrical Engineering, University College London., Torrington Place, London WC1E 7JE,UK
ssavory@ee.ucl.ac.uk

Abstract: Digital filters underpin the performance of coherent optical receivers which exploit digital signal processing (DSP) to mitigate transmission impairments. We outline the principles of such receivers and review our experimental investigations into compensation of polarization mode dispersion. We then consider the details of the digital filtering employed and present an analytical solution to the design of a chromatic dispersion compensating filter. Using the analytical solution an upper bound on the number of taps required to compensate chromatic dispersion is obtained, with simulation revealing an improved bound of 2.2 taps per 1000ps/nm for 10.7GBaud data. Finally the principles of digital polarization tracking are outlined and through simulation, it is demonstrated that 100krad/s polarization rotations could be tracked using DSP with a clock frequency of less than 500MHz.

OCIS codes: (060.1660) Coherent communications; (060.4510) Optical communications;

References and Links

1. P. S. Henry, "Lightwave Primer" IEEE J. Quantum Electron. **21**, 1862-1879 (1985)
2. H. Bülow, "Electronic dispersion compensation," *Proc. Opt. Fiber Comm. Conf. 2007*, paper OMG5
3. T. Okoshi and K. Kikuchi, "Coherent Optical Fiber Communications," KTK, 1988
4. M. G. Taylor, "Coherent detection method using DSP for demodulation of signal and subsequent equalization of propagation impairments" IEEE Photon. Technol. Lett. **16**, 674 – 676 (2004).
5. S. Tsukamoto, D.-S Ly-Gagnon, K. Katoh, and K. Kikuchi, "Coherent demodulation of 40-Gbit/s polarization-multiplexed QPSK signals with 16-GHz spacing after 200-km transmission," in Proceedings of Optical Fiber Communications Conference 2005, paper PDP-29
6. S.J. Savory, A.D. Stewart, S. Wood, G. Gavioli, M.G. Taylor, R.I. Killey, P. Bayvel, "Digital Equalisation of 40Gbit/s per Wavelength Transmission over 2480km of Standard Fibre without Optical Dispersion Compensation," in Proceedings of ECOC 2006, Cannes, France, paper Th2.5.5, Sep. 2006.
7. C.R.S. Fludger, T.Duthel, T. Wuth, C. Schulien, "Uncompensated Transmission of 86Gbit/s Polarization Multiplexed RZ-QPSK over 100km of NDSF Employing Coherent Equalisation," in Proceedings of ECOC 2006, Cannes, France, paper, Th4.3.3
8. S.J. Savory, G. Gavioli, R.I. Killey and P. Bayvel, "Electronic compensation of chromatic dispersion using a digital coherent receiver," Opt. Express **15,** 2120-2126 (2007).
9. C. Laperle, B. Villeneuve, Z. Zhang, D. McGhan, H. Sun, M. O'Sullivan, "Wavelength Division Multiplexing (WDM) and Polarization Mode Dispersion (PMD) Performance of a Coherent 40Gbit/s Dual-Polarization Quadrature Phase Shift Keying (DP-QPSK) Transceiver," in Proceedings of Optical Fiber Communications Conference 2007, paper PDP16
10. G. Charlet, J. Renaudier, M. Salsi, H. Mardoyan, P. Tran, S. Bigo "Efficient Mitigation of Fiber Impairments in an Ultra-Long Haul Transmission of 40Gbit/s Polarization-Multiplexed Data, by Digital Processing in a Coherent Receiver," in Proceedings of Optical Fiber Communications Conference 2007, paper PDP17
11. C. R. S. Fludger, T. Duthel, D. van den Borne, C. Schulien, E-D. Schmidt, T. Wuth, E. de Man, G. D. Khoe, H. de Waardt, "10 x 111 Gbit/s, 50 GHz Spaced, POLMUX-RZ-DQPSK Transmission over 2375 km Employing Coherent Equalisation," in Proceedings of Optical Fiber Communications Conference 2007, paper PDP22
12. G. Goldfarb and G. Li, "Chromatic dispersion compensation using digital IIR filtering with coherent detection," IEEE Photon. Technol. Lett. **19,** 969-971 (2007).
13. E. Ip and J.M Kahn, "Digital Equalization of Chromatic Dispersion and Polarization Mode Dispersion" J. Lightwave Technol. **25,** 2033-2043 (2007)
14. D. van den Borne, H. de Waardt, G.-D. Khoe, T. Duthel, C. R.S. Fludger, C. Schulien, E. –D. Schmidt, "Electrical PMD Compensation in 43-Gb/s POLMUX-NRZ-DQPSK enabled by Coherent Detection and Equalization," in Proceedings ECOC 2007, Berlin, Germany, invited paper 8.3.1

#87192 - $15.00 USD Received 4 Sep 2007; revised 14 Nov 2007; accepted 14 Nov 2007; published 9 Jan 2008

15. S.J. Savory, V. Mikhailov, R.I. Killey, P. Bayvel, "Digital coherent receivers for uncompensated 42.8Gbit/s transmission over high PMD fibre," in Proceedings ECOC 2007, Berlin, Germany, invited paper 10.4.1
16. A. Leven, N. Kaneda, U-V Koc, Y.-K. Chen "Frequency Estimation in Intradyne Reception," IEEE Photon. Technol. Lett. **19,** 366 - 368 (2007)
17. Q. Yu, L.-S. Yan, S. Lee, A.E. Willner, "Loop-Synchronous Polarization Scrambling for Simulating Polarization Effects Using Recirculating Fiber Loops," J. Lightwave Technol. **21,** 1593-1600 (2003)
18. S. R. Desbruslais and P. R. Morkel, "Simulation of polarization mode dispersion and its effects in long-haul optically amplified lightwave systems," IEE Colloquium on International Transmission System, 6.1-6.6 (1994).
19. M. J. D. Powell, *Approximation Theory and Methods*, Cambridge University Press, 1981.
20. S. Haykin, "Signal processing: where physics and mathematics meet," IEEE Signal Process. Mag. **18,** 6-7 (2001)
21. G.P. Agrawal, *Nonlinear Fiber Optics*, (Academic Press, 2001), Chap. 3
22. S. Betti, F. Curti, G. De Marchis and E. Iannone, "A novel multilevel coherent optical system: four quadrature signaling," J. Lightwave Technol. **9,** 514-523 (1991)
23. Y. Han and G. Li, "Coherent optical communication using polarization multiple-input-multiple-output," Opt. Express **13,** 7527-7534 (2005).
24. D. Godard, "Self-recovering equalization and carrier tracking in two-dimensional data communication systems," IEEE Trans. Commun. **28,** 1867 – 1875 (1980).
25. C.R. Johnson, P. Schniter, T.J. Endres, J.D. Behm, D.R. Brown, R.A. Casas, "Blind Equalization Using the Constant Modulus Criterion: A Review," Proc. IEEE **86,** 1927-1950 (1998)
26. J.G. Proakis, *Digital Communications*, 4th Ed., McGraw Hill, 2001
27. S. Haykin, *Adaptive Filter Theory*, 4th Ed., Prentice Hall, 2001
28. J.J. Rodriguez-Andina, M.J. Moure and M.D. Valdes, "Features, design tools, and application domains of FPGAs," IEEE Trans Ind. Electron. **54,** 1810-1823, (2007)
29. T. Pfau et al. "PDL-tolerant real-time polarization-multiplexed QPSK transmission with digital coherent polarization diversity receiver" *Proceedings of IEEE LEOS Summer Topical Meeting, 2007*, paper MA3.3

1. Introduction

Prior to the advent of dispersion compensating fiber (DCF), chromatic dispersion was considered to be one of the key limitations for optical communications systems[1]. Although current systems use DCF this increases the complexity and cost of the system with an alternative approach being to compensate the chromatic dispersion entirely in the electrical domain either at the transmitter or receiver. Of the options considered for electronic chromatic dispersion compensation, one of the most promising is a phase and polarisation diverse digital coherent receiver[2].

While coherent detection was experimentally demonstrated as early as 1979[3], its use in commercial systems has been hindered by the additional complexity, due to the need to track the phase and the polarization of the incoming signal. In a digital coherent receiver these functions are implemented in the electrical domain leading to a dramatic reduction in complexity. Furthermore since coherent detection maps the entire optical field within the receiver bandwidth into the electrical domain it maximizes the efficacy of the signal processing. This allows impairments which have traditionally limited 40Gbit/s systems to be overcome, since both chromatic dispersion and polarization mode dispersion (PMD) may be compensated adaptively using linear digital filters[4-15].

This paper consists of three parts. Firstly we outline the principles of a digital coherent receiver and demonstrate its ability to compensate large values of PMD. We then present a new method for the design of the chromatic dispersion compensating filter, which allows bounds to be obtained on the performance of such a filter. Finally we consider the dynamical behavior of the receiver, in order to estimate the speed at which polarization rotations could be tracked. While the focus of this paper will be 40Gbit/s systems the principles described are equally applicable to higher data rates such as 100Gbit/s and beyond.

2. Principles of digital coherent receivers

2.1 Receiver architecture

Digital coherent receivers utilize a phase and polarization diverse architecture to map the optical field into the electrical domain. Once digitized, digital signal processing (DSP), is used

#87192 - $15.00 USD Received 4 Sep 2007; revised 14 Nov 2007; accepted 14 Nov 2007; published 9 Jan 2008

to track both the phase and polarization of the signal, allowing for a considerable reduction in complexity compared to an optical homodyne receiver. The functionality of the phase and polarization diverse coherent receiver is to map in the optical field into four electrical signals, corresponding to the in-phase and quadrature field components for the two polarizations. This may be achieved practically using a number of options, ranging from more complex options such as the passive quadrature hybrid with balanced detectors to fused fiber couplers with single ended photodiodes as illustrated in Fig. 1.

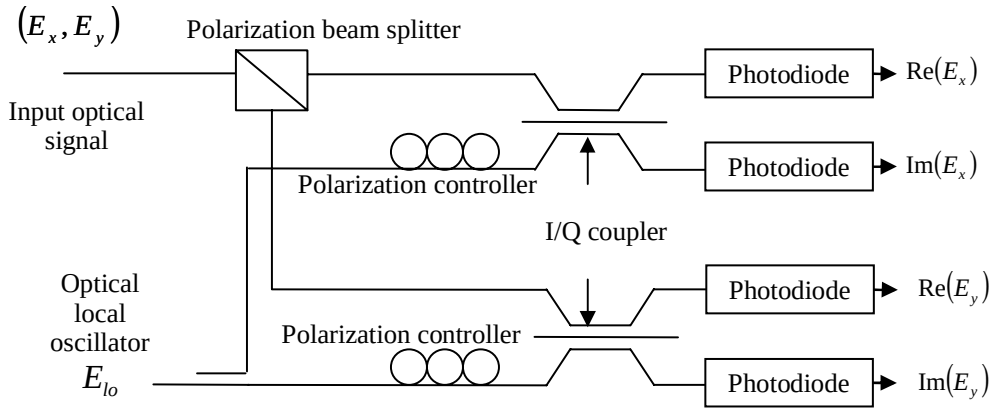

Fig. 1. Schematic of a phase and polarization diverse receiver where E_x, E_y and E_{lo} are the electric fields associated with the horizontal and vertical polarization components of the input optical signal and local oscillator respectively

The exact details of architecture chosen to implement the phase and polarization diverse receiver will have little bearing on the subsequent DSP. Therefore without loss of generality, as in our previous experimental work[8], we consider the architecture illustrated in Fig. 1, in which asymmetric 3x3 fiber couplers are employed as 90° hybrids, such that the four electrical signal are given by

$$\begin{pmatrix} i_1 \\ i_2 \\ i_3 \\ i_4 \end{pmatrix} = \frac{2}{5} \underbrace{\begin{pmatrix} \mathrm{Re}\left(E_x E_{lo}^*\right) \\ \mathrm{Im}\left(E_x E_{lo}^*\right) \\ \mathrm{Re}\left(E_y E_{lo}^*\right) \\ \mathrm{Im}\left(E_y E_{lo}^*\right) \end{pmatrix}}_{\text{coherent terms}} + \frac{1}{10} \underbrace{\begin{pmatrix} 2|E_x|^2 + 2|E_{lo}|^2 \\ 4|E_x|^2 + |E_{lo}|^2 \\ 2|E_y|^2 + 2|E_{lo}|^2 \\ 4|E_y|^2 + |E_{lo}|^2 \end{pmatrix}}_{\text{direct detection terms}} \tag{1}$$

The directly detected local oscillator power may be removed using a DC block, and the remaining terms may be minimized by ensuring that the ratio of the local oscillator to the signal is significantly larger than the signal to noise ratio of interest. In practice for systems which employ forward error correction (FEC) this corresponds to an LO/signal ratio in the region of 20dB.

2.2 Outline of the digital signal processing

The role of the digital signal processing is to reconstruct the transmitted data from the received signal, and has several stages such as those detailed in Fig. 2. The first three blocks for the signal processing, are fundamentally concerned with signal conditioning, such that after these blocks the four channels are synchronized with an integer number of samples per symbol, with the normalization and orthogonalization sub-block compensating for imperfections in the 90° hybrid and the variation of the responsitivity of the four photodiodes.

#87192 - $15.00 USD Received 4 Sep 2007; revised 14 Nov 2007; accepted 14 Nov 2007; published 9 Jan 2008

Following this digital filtering occurs to compensate polarization rotations and transmission impairments after which the phase and frequency mismatch between the incoming signal and the local oscillator is then compensated using algorithms such as those detailed in [8,16] before the data is finally recovered and FEC applied. The focus of this paper is the digital filtering stage which we now discuss in more detail.

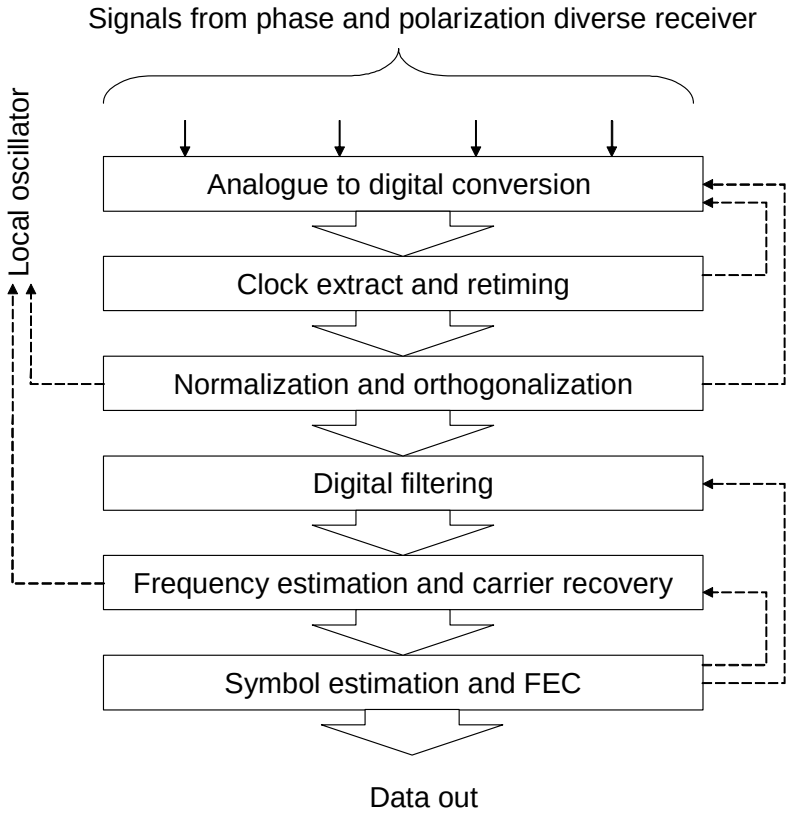

Fig. 2. Schematic of the DSP blocks in a digital coherent receiver

2.3 Functionality of the digital filtering

In order to efficiently compensate for transmission impairments it is often beneficial to partition the functionality of the digital filtering into two blocks as illustrated in Fig. 3. The first of these blocks compensates for polarization independent impairments such as chromatic dispersion, with the second compensating for polarization dependent effects such polarization rotations and PMD. The partitioning of the digital filtering allows the two blocks to adapt at different rates, for example on a millisecond timescale the chromatic dispersion may be viewed as constant, whereas the polarization may vary. Furthermore it allows for large amounts of chromatic dispersion to be compensated without the need to frequently adapt the tap weights which has significant advantages for the implementation of the DSP.

If nonlinear impairments such as self phase modulation or nonlinear phase noise are to be compensated, additional nonlinear filtering will be required. In this paper however, we shall restrict the discussion to linear digital filtering which may be implemented using the architecture of Fig. 3. This architecture is well suited to the compensation linear transmission impairments due to chromatic dispersion and PMD, with the additional advantage that the filters can be implemented in either directly in the time domain or using fast convolution techniques in the frequency domain in order to minimize the overall DSP complexity.

#87192 - $15.00 USD Received 4 Sep 2007; revised 14 Nov 2007; accepted 14 Nov 2007; published 9 Jan 2008

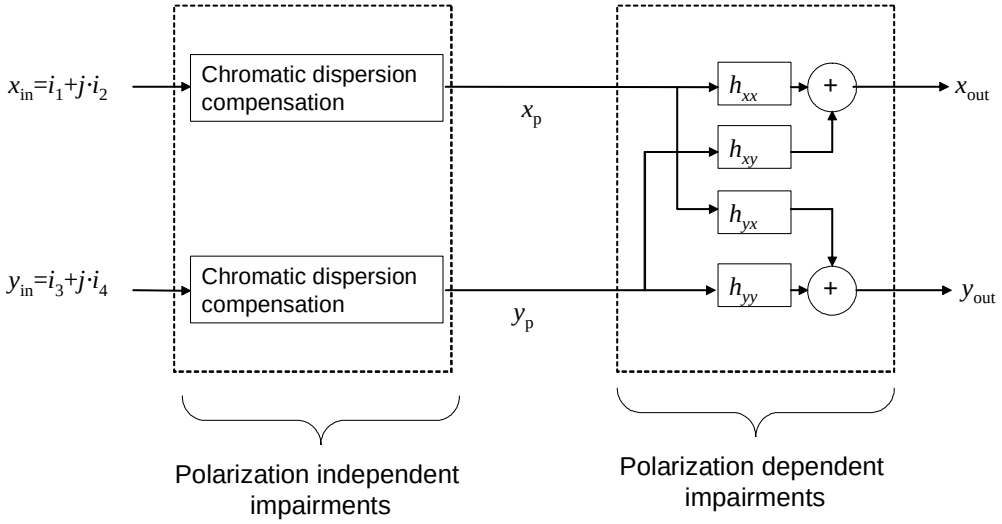

Fig. 3. Functionality of the digital filtering stage. For linear filtering the order of the two sub-blocks may of course be reversed

2.4 Knowledge of the signal alphabet

To maximize the efficacy of the DSP, it is beneficial to exploit the finite alphabet of symbols over which the data is transmitted. Given we are able to receive the four components of the electric field, the efficiency of the receiver is maximized when each one of these components carries data. The simplest option is thus to modulate binary on each dimension, which corresponds to polarization division multiplexed QPSK (PDM-QPSK). This modulation format has the property that in the absence of distortion the two QPSK channels are of constant modulus, a feature which can be exploited by the DSP.

3. Application to the compensation of polarization mode dispersion

In order to demonstrate the power of the techniques which will discuss in the subsequent sections, we review our recent experimental investigations into the compensation of PMD[15] which is a major concern for 40Gbit/s systems as well as 10Gbit/s data transmitted over legacy fiber with high PMD. To investigate the relationship between PMD and bit error rate (BER) we inserted a fixed differential group delay (DGD) per recirculation which, combined with a loop synchronous polarisation scrambler, ensured that the resulting PMD had all orders, with the first order DGD having a Maxwellian distribution[17]. Using the standard formula for the waveplate model[18] the mean DGD (<DGD>) is given by

$$\langle DGD \rangle = \text{DGD per loop} \times \sqrt{\frac{8}{3\pi} \times \text{number of recirculations}} \tag{2}$$

All measurements were performed after 40 recirculations such that the mean DGD is given by <DGD>=5.83 x DGD per loop. As in our previous work[8] the weights of the 512 taps used in the chromatic dispersion compensating filter were calculated from a truncated impulse response obtained using a frequency sampling technique with a Kaiser window function. Due to the increased amount of PMD however the number of taps used in the adaptive equalizer was increased to 13 taps. The set up of the recirculating loop experiment is illustrated in Fig. 4 in which the data was transmitted as 42.8Gbit/s using 10.7GBaud PDM-QPSK. The electrical waveforms are captured by a digital storage oscilloscope after 40 recirculations generating an accumulated dispersion of 53,712ps/nm at the receiver after transmitting over 3200km of

#87192 - $15.00 USD Received 4 Sep 2007; revised 14 Nov 2007; accepted 14 Nov 2007; published 9 Jan 2008

G.652 fiber. The DGD per recirculation was increased from 0 to 32ps in steps of 4ps, corresponding to changing the mean PMD after 40 recirculations from 0 to 186ps in steps of 23.3ps. For each value of DGD, ten independent measurements were carried out in order to explore the statistical variation of DGD, with further details of the experimental setup being given in [15].

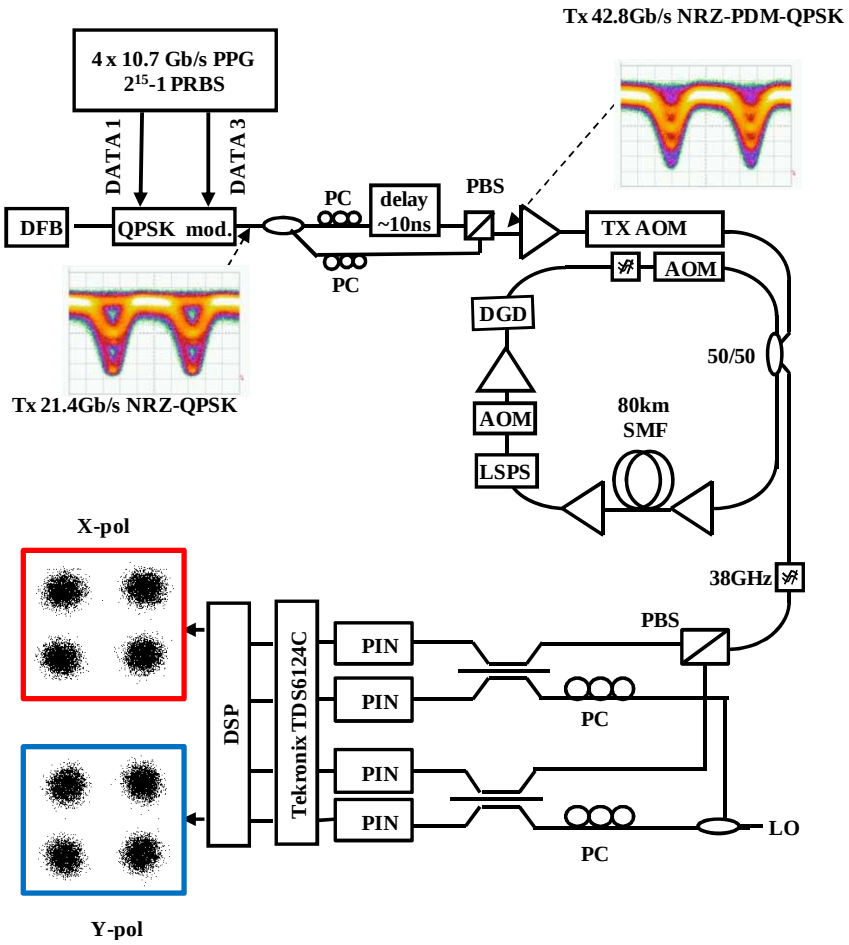

Fig. 4. Experimental setup of the recirculating loop experiment full details of which are given in [15]. Recovered constellations are obtained with 100ps mean DGD (32ps/loop) and 53,712ps/nm chromatic dispersion from 3200km fibe

3.2 Experimental transmission results

In each case the BER was measured over 131,068 bits, with $Q=\sqrt{2}\times\text{erfcinv}(2\times BER)$ determined from the mean BER obtained for each value of DGD. These results are plotted in Fig. 5 (left), along with a quadratic fit, given by $20\log_{10}Q=10.9-8.63\times10^{-6}\times\langle DGD\rangle^2$ where the parameters have been obtained by minimizing the L_1 norm (mean absolute error) since this is insensitive to extreme outliers[19]. These results indicate an expected penalty of 0.1dBQ for 100ps mean DGD, increasing to 0.3dBQ for 186ps mean DGD.

To further investigate the statistical nature of the BER when randomly distributed DGD was present, we performed 100 measurements for two cases. Firstly, this was done when there was no PMD added, and secondly when the mean DGD was 100 ps (corresponding to a DGD of 18ps/recirculation), with the BER was measured over 262,136 bits. To investigate the

#87192 - $15.00 USD Received 4 Sep 2007; revised 14 Nov 2007; accepted 14 Nov 2007; published 9 Jan 2008

statistical nature, we determined the mean and variance for the two cases, being $\mu=2.4\times10^{-4}$ and $\sigma^2=2.0\times10^{-9}$ for zero DGD and $\mu=2.7\times10^{-4}$ and $\sigma^2=2.8\times10^{-9}$ for 100ps mean. For each set of data an approximate probability density function (pdf) was obtained by dividing the BER data into bins. As can be seen in Fig. 5 (right) there is good agreement between the approximate pdf of the BER and the fitted Gaussian distribution for the two cases. There is only a slight difference between the pdfs for the case with no PMD and that with 100 ps mean DGD, indicating for all of the cases considered the PMD has been compensated with minimal impact on performance. In order to quantify the penalty we note that change in the mean BER from 2.4×10^{-4} to 2.7×10^{-4} corresponds to a change of $20\log_{10}Q$ of less than 0.1 dB, in agreement with that expected from the quadratic L_1 fit displayed in Fig. 5 (left).

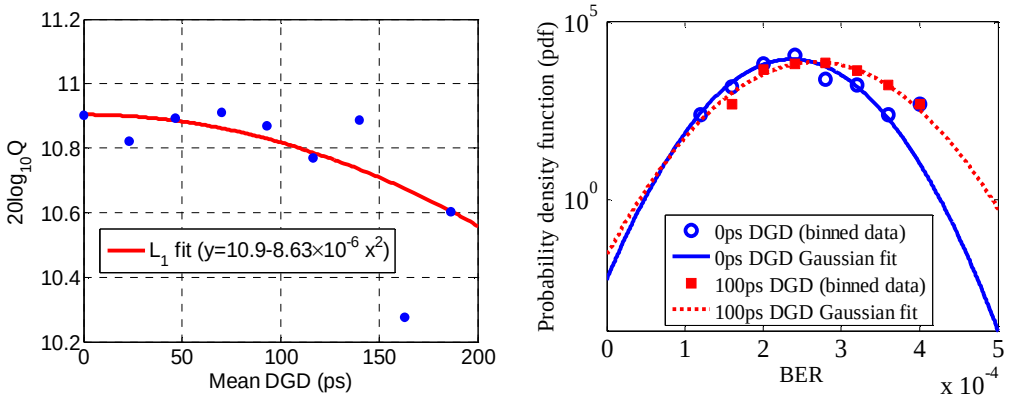

Fig 5. The impact of PMD on the performance (left), and the pdf of the BER (right)

As can be seen the DGD is very effectively compensated which provides suitable motivation for the study of the digital filtering employed.

4. Compensation of chromatic dispersion

4.1 The design of dispersion compensating filters

In the transmission experiment outlined in the previous section in excess of 50,000ps/nm of chromatic dispersion is compensated while simultaneously compensating for the PMD. This may however be extended further, with our previous experimental investigations into the nonlinear tolerance of 42.8Gbit/s PDM-QPSK demonstrating compensation of more than 100,000ps/nm of chromatic dispersion generated by 6400km of standard fiber[8]. Key to achieving these results is the design of the dispersion compensating filter, a topic which we will now address.

While generic methods such as the Wiener filter may be used[13], they do not exploit our knowledge of the physics of the optical fiber. As noted by Haykin "Signal processing is at its best when it successfully combines the unique ability of mathematics to generalize with both the insight and prior information gained from the underlying physics of the problem at hand"[20]. Therefore in order to compensate chromatic dispersion, we shall begin by considering the physics of chromatic dispersion.

In the absence of fiber nonlinearity, the resulting system is linear, and the effect of chromatic dispersion on the envelope $A(z,t)$ of a pulse may be modeled by the following partial differential equation[21]

$$\frac{\partial A(z,t)}{\partial z} = j\frac{D\lambda^2}{4\pi c}\frac{\partial^2 A(z,t)}{\partial t^2} \tag{3}$$

where z is the distance of propagation, t is time variable in a frame moving with the pulse, $j=\sqrt{-1}$, λ is the wavelength of the light, c is the speed of light, and D is the dispersion coefficient of the fiber.

#87192 - $15.00 USD Received 4 Sep 2007; revised 14 Nov 2007; accepted 14 Nov 2007; published 9 Jan 2008

The conventional approach is to take the Fourier transform of Eq. (3) and solve to give the frequency domain transfer function $G(z,\omega)$ given by

$$G(z,\omega) = \exp\left(-j\frac{D\lambda^2}{4\pi c}\omega^2\right) \tag{4}$$

where ω is the angular frequency. The dispersion compensating filter is therefore given by the all-pass filter $1/G(z,\omega)$, which can be approximated using nonrecursive[4,8] or recursive[12] digital filters. In both cases however the design is nontrivial, for example, in theory an all-pass filter can only be created using a recursive filter, however, it is not possible to design such a filter with the desired phase response[12]. Herein we will present, a time domain approach to the design of the chromatic dispersion compensating filter. In contrast to the frequency domain approach we previously used[8], not only does this give a simple closed form solution for the tap weights but also it provides bounds on the number of taps required for a given value of dispersion.

4.2 Time domain design of the chromatic dispersion compensating filter

Using Fourier transforms Eq. (4) maybe inverted to give the impulse response of the dispersive fiber as

$$g(z,t) = \sqrt{\frac{c}{jD\lambda^2 z}}\exp\left(j\frac{\pi c}{D\lambda^2 z}t^2\right) \tag{5}$$

For an arbitrary input, the output can be obtained by convolving this impulse response with the input and as expected the impulse response itself satisfies Eq. (3). By inverting the sign of the chromatic dispersion we obtain the impulse function of the chromatic dispersion compensating filter $g_C(z,t)$, given by

$$g_C(z,t) = \sqrt{\frac{jc}{D\lambda^2 z}}\exp\left(-j\phi(t)\right) \text{ where } \phi(t) = \frac{\pi c}{D\lambda^2 z}t^2 \tag{6}$$

The impulse response given by Eq. (6) presents a number of issues for digital implementation, not only is it infinite in duration and non-causal, but since it passes all frequencies for a finite sampling frequency aliasing will occur. The solution to all of these problems is to truncate the impulse response to a finite duration. To determine the length of the truncation window we note that if we sample every T seconds then aliasing will occur for frequencies which exceed the Nyquist frequency given by $\omega_n = \pi/T$ and that the impulse response may be considered as a rotating vector whose angular frequency is given by

$$\omega = \frac{\partial\phi(t)}{\partial t} = \frac{2\pi c}{D\lambda^2 z}t \tag{7}$$

When the magnitude of this frequency exceeds the Nyquist frequency, aliasing will occur, giving the criterion that

$$-\frac{|D|\lambda^2 z}{2cT} \le t \le \frac{|D|\lambda^2 z}{2cT} \tag{8}$$

Since the impulse response is of finite duration, we can implement this digitally using a finite impulse response (FIR) filter, which has a non-recursive structure and may be implemented using a tapped delay line. If we assume the number of taps is large then the sampled impulse response will approximate the continuous time impulse response. Hence if we consider an odd number of taps such that the total number of taps is N, then the tap weights will be given by

$$a_k = \sqrt{\frac{jcT^2}{D\lambda^2 z}}\exp\left(-j\frac{\pi cT^2}{D\lambda^2 z}k^2\right) \quad -\left\lfloor\frac{N}{2}\right\rfloor \le k \le \left\lfloor\frac{N}{2}\right\rfloor \text{ and } N = 2\times\left\lfloor\frac{|D|\lambda^2 z}{2cT^2}\right\rfloor + 1 \tag{9}$$

#87192 - $15.00 USD Received 4 Sep 2007; revised 14 Nov 2007; accepted 14 Nov 2007; published 9 Jan 2008

where $\lfloor x \rfloor$ is the integer part of x rounded towards minus infinity. These tap weights form the basis for the compensation of chromatic dispersion using an FIR filter. It should however be noted that this is an upper bound on the number of taps, with the resulting filter attempting to give constant dispersion over the frequency range $-0.5/T \le f \le 0.5/T$, and that in practice the number of taps may be reduced in order to give constant dispersion over a reduced frequency range. Furthermore properties of the filter, such as group delay ripple, maybe improved by windowing this analytical finite impulse function.

Using Eq. (9) it can be seen that if we operate in the 1550 nm transmission window and have two samples per symbol with a Baud rate of B GBaud, then the number of taps per 1000 ps/nm of chromatic dispersion will be given by $N = 0.032B^2$. Thus for a 10.7 Gbaud system transmitting over 4000km of standard fiber with D=17ps/nm/km this would require no more than 250 taps.

4.3 Numerical investigation of the compensation of chromatic dispersion

To illustrate the methods outlined we consider compensation of chromatic dispersion from a fiber with a dispersion coefficient D=17 ps/nm/km. The modulation format is PDM-QPSK, operating at 42.8Gbit/s with a 2^{15}-1 PRBS, such that the symbol rate is 10.7GBaud with λ=1553nm. This is filtered by a 7GHz 5th order Bessel filter to reduce the noise and prevent aliasing after which the signal is sampled at 21.4GSa/s. The signal is then digital filtered after which the bit error rate (BER) is measured over a total of 262136 bits. The frequency offset between the local oscillator and the signal is set to zero, and the phase noise of the lasers is neglected, however since the equalizer is invariant to phase noise this omission will not affect the conclusions. The system is considered linear with noise applied at the receiver and the impact of quantization is not included.

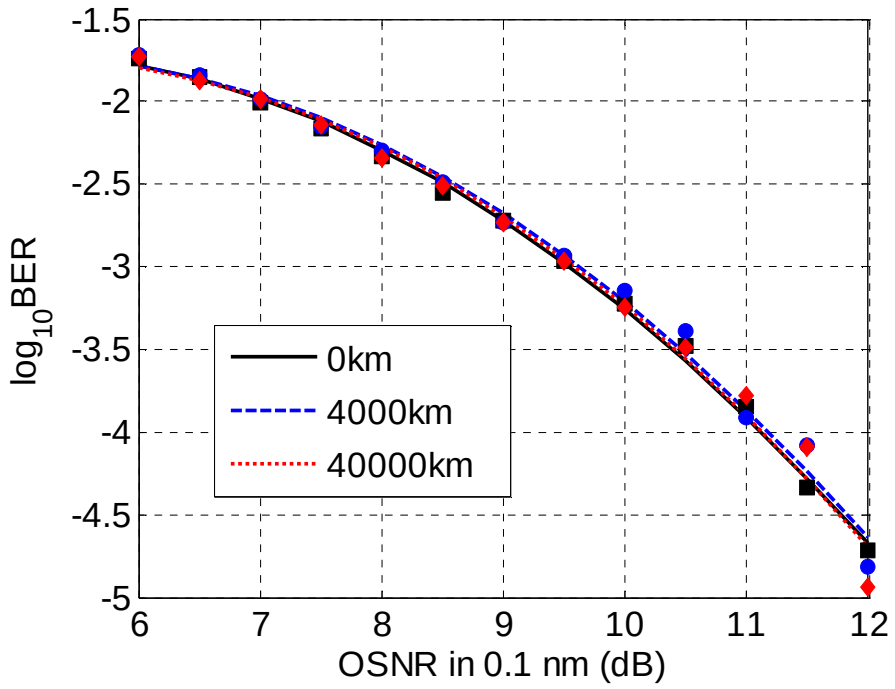

Fig. 6. BER as a function of OSNR for 0km, 4000km (251 taps) and 40000km (2501 taps)

In Fig. 6 we have compared the results for back to back (0km) and after a chromatic dispersion corresponding to 4000km and 40,000km, generating 68,000ps/nm and 680,000ps/nm of chromatic dispersion respectively. As can be seen from Fig. 6, there is no

#87192 - $15.00 USD Received 4 Sep 2007; revised 14 Nov 2007; accepted 14 Nov 2007; published 9 Jan 2008

notable penalty associated with the compensation of arbitrarily large amounts of chromatic dispersion when the maximal truncation window given by Eq. (9) is employed, giving an asymptotic limit of 3.7 taps per 1000ps/nm of chromatic dispersion for this 10.7GBaud system. To realize such a filter practically, it is desirable to minimize the number of tap without compromising performance. In order to generalize our findings, we normalize the number of taps by the length of the maximal truncation window filter given by Eq. (9). As indicated in the results displayed in Fig. 7 as we reduce the number of taps the performance decreases however significant reductions in the number of taps can be achieved with minimal impact on performance. In the cases considered the normalized number of taps can be reduced to 60% with a penalty of less than 0.25dBQ giving an asymptotic limit of 2.2 taps per 1000ps/nm of chromatic dispersion, with the reduction being comparable to that expected from the ratio of the 7GHz signal bandwidth to the 10.7GHz Nyquist frequency. While the taps weights may be suboptimal when the number of taps is less than the maximal truncation window, they provide a basis for further optimization.

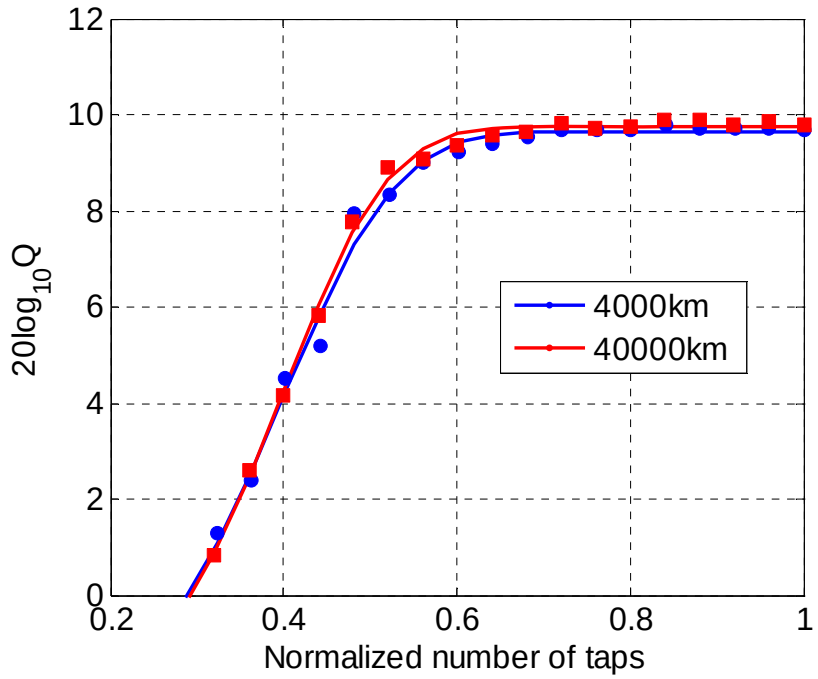

Fig. 7. Performance with OSNR=9.5dB of Q=√2erfcinv(2BER) versus normalized number of taps being the ratio of the number of taps to the maximal truncation window given by Eq. (9)

5. Compensation of polarization dependent effects

5.1 Obtaining the inverse Jones matrix of the channel

The impact of polarization dependent effects on the propagation may be modeled by a Jones matrix. In general this matrix is not unitary due to polarization dependent loss (PDL) and furthermore it will be frequency dependent due to polarization mode dispersion (PMD). The task is therefore to estimate the Jones matrix and obtain the inverse to compensate for the impairments incurred. In contrast to the chromatic dispersion which may be considered constant, the Jones matrix may evolve in time due to effects such as rapid variations in the polarization state, and therefore the compensation scheme must be adaptive. The problem of compensating polarization rotations digitally was first considered by Betti et al[22], and later

#87192 - $15.00 USD Received 4 Sep 2007; revised 14 Nov 2007; accepted 14 Nov 2007; published 9 Jan 2008

demonstrated utilizing the formalism of multiple input multiple output (MIMO) systems[8,23]. For inputs $x_p(k)$ and $y_p(k)$ the output $x_{out}(k)$ is given by

$$x_{out}(k) = \mathbf{h}_{xx}^T \cdot \mathbf{x}_p + \mathbf{h}_{xy}^T \cdot \mathbf{y}_p = \sum_{m=0}^{M-1} h_{xx}(m)x_p(k-m) + h_{xy}(m)y_p(k-m) \tag{10}$$

and likewise $y_{out}(k) = \mathbf{h}_{yx}^T \cdot \mathbf{x}_p + \mathbf{h}_{yy}^T \cdot \mathbf{y}_p$, where $\mathbf{h_{xx}}$, $\mathbf{h_{xy}}$, $\mathbf{h_{yx}}$, $\mathbf{h_{yy}}$ are adaptive filters each of which have length M taps. While there are a number of methods for adapting the equalizer in MIMO systems, we shall restrict ourselves to a specific example that exploits properties of the data, namely that for polarization division multiplexed QPSK (PDM-QPSK) the signal for each polarization should have a constant modulus[24]. This constant modulus algorithm (CMA), has also been shown to be effective even when the modulus is not constant such as higher order quadrature amplitude modulation[24,25].

5.2 Update algorithm for the adaptive equalizer

For signals of unit amplitude the equalizer will attempt to minimize, in a mean squares sense, the magnitude of $\varepsilon_x = 1 - |x_{out}|^2$ and $\varepsilon_y = 1 - |y_{out}|^2$, giving the following criteria

$$\frac{d\langle \varepsilon_x^2 \rangle}{d\mathbf{h}_{xx}} = 0 \; ; \; \frac{d\langle \varepsilon_x^2 \rangle}{d\mathbf{h}_{xy}} = 0 ; \; \frac{d\langle \varepsilon_y^2 \rangle}{d\mathbf{h}_{yx}} = 0 ; \; \frac{d\langle \varepsilon_y^2 \rangle}{d\mathbf{h}_{yy}} = 0 \tag{11}$$

To determine the optimal tap weights, the gradients are replaced by their instantaneous values resulting in the a set of stochastic gradient algorithms with convergence parameter μ

$$\mathbf{h}_{xx} \to \mathbf{h}_{xx} - \frac{\mu}{4}\frac{d\varepsilon_x^2}{d\mathbf{h}_{xx}} = \mathbf{h}_{xx} + \mu\varepsilon_x x_{out} \cdot \overline{\mathbf{x}}_p \tag{12}$$

$$\mathbf{h}_{xy} \to \mathbf{h}_{xy} - \frac{\mu}{4}\frac{d\varepsilon_x^2}{d\mathbf{h}_{xy}} = \mathbf{h}_{xy} + \mu\varepsilon_x x_{out} \cdot \overline{\mathbf{y}}_p \tag{13}$$

$$\mathbf{h}_{yx} \to \mathbf{h}_{yx} - \frac{\mu}{4}\frac{d\varepsilon_y^2}{d\mathbf{h}_{yx}} = \mathbf{h}_{yx} + \mu\varepsilon_y y_{out} \cdot \overline{\mathbf{x}}_p \tag{14}$$

$$\mathbf{h}_{yy} \to \mathbf{h}_{yy} - \frac{\mu}{4}\frac{d\varepsilon_y^2}{d\mathbf{h}_{yy}} = \mathbf{h}_{yy} + \mu\varepsilon_y y_{out} \cdot \overline{\mathbf{y}}_p \tag{15}$$

where $\overline{\mathbf{x}}_p$ and $\overline{\mathbf{y}}_p$ denotes the complex conjugate of $\mathbf{x}_p$ and $\mathbf{y}_p$ respectively. In order to initialize the algorithm, all tap weights are set to zero with the exception of the central tap of $\mathbf{h}_{xx}$ and $\mathbf{h}_{yy}$ which are set to unity. Given the equalizer is unconstrained with respect to its outputs, it is possible for the equalizer to converge on the same output, corresponding to the Jones matrix becoming singular. This may however he remedied by monitoring the determinant of the Jones matrix such that if it begins to approach zero then the equalizer is re-initialized with tap weights $\mathbf{h}_{xx}(k) \to 0.5\left(\mathbf{h}_{xx}(k) + \overline{\mathbf{h}}_{yy}(M-1-k)\right)$, $\mathbf{h}_{yy}(k) \to \overline{\mathbf{h}}_{xx}(M-1-k)$ $\mathbf{h}_{xy}(k) \to 0.5\left(\mathbf{h}_{xy}(k) - \overline{\mathbf{h}}_{yx}(M-1-k)\right)$, $\mathbf{h}_{yx}(k) \to -\overline{\mathbf{h}}_{xy}(M-1-k)$ where $k = 0,1..M-1$.

Once the equalizer has converged, then the equalizer may move into a decision directed mode, using a decision directed least mean squared (DD-LMS) algorithm such that[26].

#87192 - $15.00 USD Received 4 Sep 2007; revised 14 Nov 2007; accepted 14 Nov 2007; published 9 Jan 2008

$$\mathbf{h}_{xx} \to \mathbf{h}_{xx} - \frac{\mu}{2}\frac{d|\varepsilon_x|^2}{d\mathbf{h}_{xx}} = \mathbf{h}_{xx} + \mu\varepsilon_x \cdot \bar{\mathbf{x}}_p \tag{16}$$

$$\mathbf{h}_{xy} \to \mathbf{h}_{xy} - \frac{\mu}{2}\frac{d|\varepsilon_x|^2}{d\mathbf{h}_{xy}} = \mathbf{h}_{xy} + \mu\varepsilon_x \cdot \bar{\mathbf{y}}_p \tag{17}$$

$$\mathbf{h}_{yx} \to \mathbf{h}_{yx} - \frac{\mu}{2}\frac{d|\varepsilon_y|^2}{d\mathbf{h}_{yx}} = \mathbf{h}_{yx} + \mu\varepsilon_y \cdot \bar{\mathbf{x}}_p \tag{18}$$

$$\mathbf{h}_{yy} \to \mathbf{h}_{yy} - \frac{\mu}{2}\frac{d|\varepsilon_y|^2}{d\mathbf{h}_{yy}} = \mathbf{h}_{yy} + \mu\varepsilon_y \cdot \bar{\mathbf{y}}_p \tag{19}$$

Where $\varepsilon_x = d_x - x_{out}$ and $\varepsilon_y = d_y - y_{out}$, with d_x and d_y and being the symbols closest to x_{out} and y_{out} respectively.

5.3 Dynamic response of the adaptive equalizer

In order to gain insight into the dynamical behavior of the equalizer structure discussed in section 3, we simulate detection following an endless polarization rotation with Jones matrix

$$J = \begin{pmatrix} \cos\omega t & \sin\omega t \\ -\sin\omega t & \cos\omega t \end{pmatrix} \tag{20}$$

where ω is the angular frequency. The four FIR filters in the equalizer each had 3 taps, with the signal noise loaded to an OSNR of 9.5dB, being commensurate with a BER of 10^{-3}.

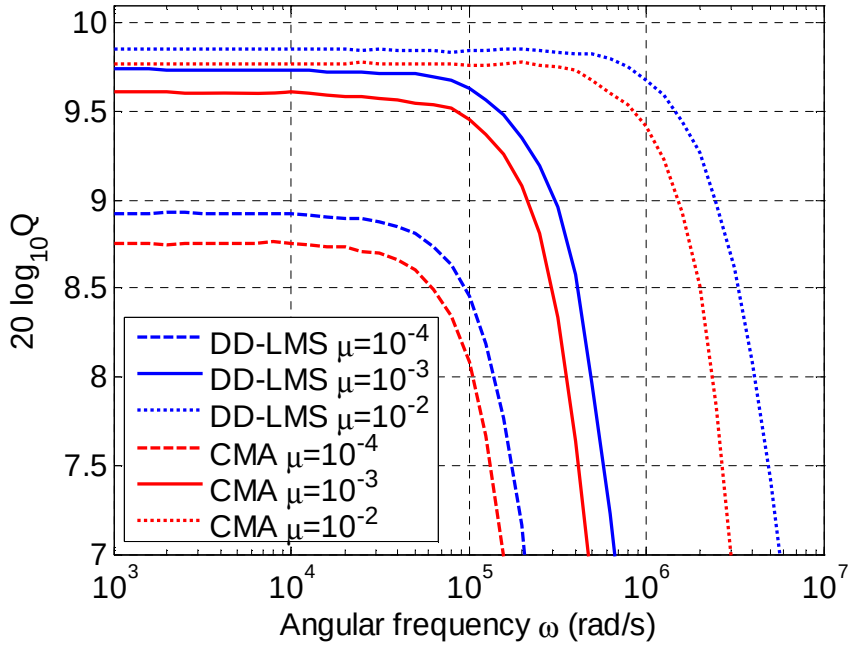

Fig. 8. Frequency response of Q using the constant modulus algorithm (red), and the decision directed least mean squares algorithm (blue) for several values of convergence parameter with 3 taps in each MIMO filter

#87192 - $15.00 USD Received 4 Sep 2007; revised 14 Nov 2007; accepted 14 Nov 2007; published 9 Jan 2008

As can be seen from Fig. 8 the dynamical behavior of the CMA and the DD-LMS algorithms are similar, albeit that in all cases the DD-LMS has a better performance than the CMA. The results indicate that with $\mu = 0.01$ it is possible to track angular frequencies of approximately 1 Mrad/s with a penalty of less than 0.5dBQ.

However in our experimental investigation into PMD compensation 13 taps were used, a number which has also been used by other groups[11]. Since the tracking performance of the classical LMS algorithm is affected by the number of taps[27], we investigate the impact of increasing the number of taps on the convergence in the absence of PMD. As can be seen from Fig. 9 the behavior of the CMA and DD-LMS are again similar. This is of particular interest since it allows the dynamical behavior to be characterized by only considering the DD-LMS which has a simpler form and lends itself to analytical study.

Of note is that the performance is improved using a 13 tap filter compared to a 3 tap filter, however if we require similar levels of performance to the case with 3 taps we can again track frequencies in the range of 1 Mrad/s.

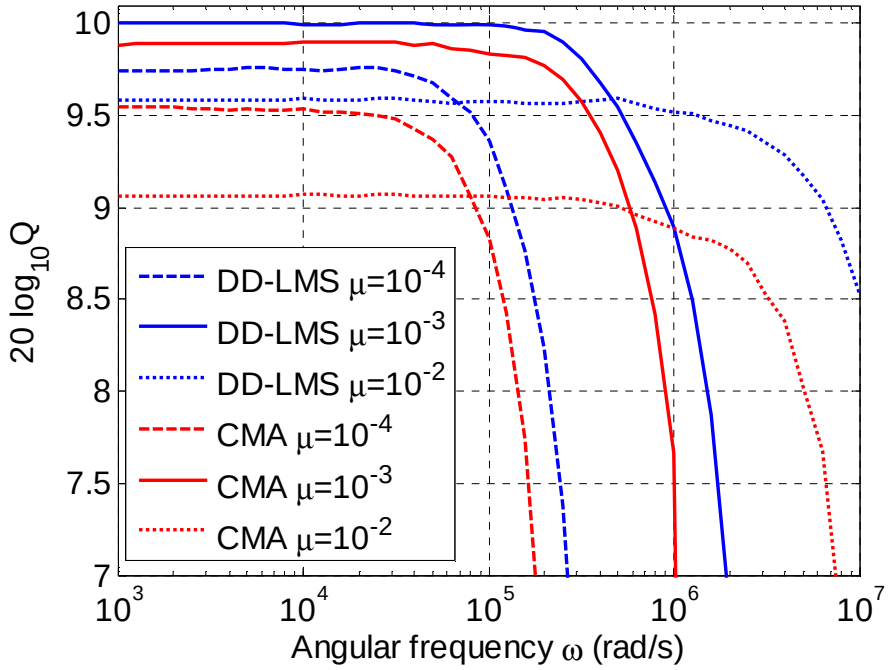

Fig. 9. Frequency response of Q using the constant modulus algorithm (red), and the decision directed least mean squares algorithm (blue) for several values of convergence parameter with 13 taps in each MIMO filter

In order to track a frequency of 1 Mrad/s it is assumed that it is possible to update the taps at the symbol rate. In contrast current DSP chips have a system clock in the region of 500 MHz[28] and therefore cannot update at the symbol frequency. To investigate the impact of decreasing the update rate of the equalizer we consider a 13 tap equalizer, and investigate updating the gradient estimate every 16, 32 and 64 symbols, corresponding to clock frequencies of 669MHz, 334MHz and 167MHz respectively. For each frequency the convergence parameter was optimized for a 1 krad/s rotation, and this value was then used for all frequencies. As can be seen in Fig. 10, for DSP with clock frequencies in the range of 500MHz polarization fluctuations in the region of 100krad/s could be tracked which is significantly higher than the 50rad/s tracking rate recently reported[29]

#87192 - $15.00 USD Received 4 Sep 2007; revised 14 Nov 2007; accepted 14 Nov 2007; published 9 Jan 2008

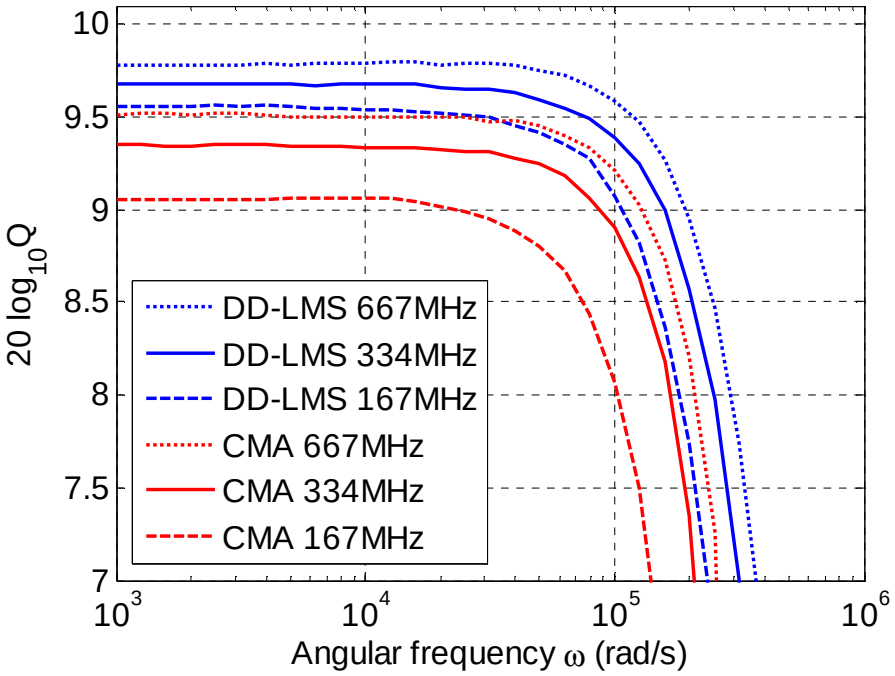

Fig. 10. Impact the update rate on a MIMO equalizer with 13 taps

From these studies it is clear that the exact choice of the algorithm and its implementation will impact the dynamical behavior of the adaptive equalizer. It should however be noted that the algorithms used are fundamentally designed to converge to the required inverse Jones matrix, which it is assumed is constant. Nevertheless using these algorithms we have demonstrated their ability to track polarization changes, however they may be sub-optimal for tracking faster polarization changes, which would require the dynamical nature of the Jones matrix the be taken into account.

6. Conclusions

Digital filtering combined with coherent detection is a powerful combination, enabling uncompensated transmission of 40Gbit/s data over high PMD fiber. The analytical truncated impulse response method for the design a digital FIR filter allows compensation of arbitrary amounts of chromatic dispersion and provides an asymptotic upper bound of 3.7 taps per 1000ps/nm of chromatic dispersion at 10.7Gbaud. Detailed simulations reveal that for a 0.25dBQ penalty this asymptotic efficiency may be improved to 2.2 taps per 1000ps/nm. The principles of digital polarization tracking have been outlined and the dynamics investigated. This reveals that the constant modulus algorithm and the decision directed algorithm have similar dynamical behavior. If the taps are updated at the maximum rate, corresponding to the baud rate then polarization rotations of 1 Mrad/s could be tracked. In practice however this will not occur due to the limits of the DSP employed. Nevertheless simulation indicates the algorithms should be capable of tracking polarization fluctuations in the region of 100krad/s for 10GBaud systems using current DSP clock rates.

Acknowledgments

Financial support from the Leverhulme Trust is gratefully acknowledged as is that received for the project from FP6 IST-IP NOBEL and EPSRC. Prof. P Bayvel, Dr. V Mikhailov, Dr. R Killey, P Watts and DS Millar are thanked for valuable discussions.

#87192 - $15.00 USD Received 4 Sep 2007; revised 14 Nov 2007; accepted 14 Nov 2007; published 9 Jan 2008